ISSN 1330-3651 (Print), ISSN 1848-6339 (Online) https://doi.org/10.17559/TV-20231020001040
Original scientific paper

Experimental and Numerical Investigation of the Tendon Layout Effect on Flexural Capacity in Post-Tensioning Beams

R. Kadir PEKGÖKGÖZ*, Gamze İZOL, Fatih AVCİL, M. Arif GÜREL

Abstract: This study examined the bending and ductility capacities of reinforced concrete beams produced with the post-tensioning technique used to cross wide spans in structures. For this purpose, six beam specimens were produced. Two of these specimens (NB/1-2) were made of normal reinforced concrete and the other four were created by applying the post-tensioning technique. The steel post-tensioning tendons of two of these specimens (POSTTENST/1-2) were placed straight along the beam, and the other beam specimens (POSTTENP/1-2) were placed parabolically. Four-point bending tests were carried out on beam specimens. As a result of the experiments, it was determined that beams strengthened with straight and parabolic steel tendons could carry approximately 62% more load and behave approximately 65% more ductile than unstrengthened beams. In the study, finite element models of the beam specimens were created and analyzed using the Abaqus program. In the parametric analysis, it was determined that as the ratio of the beam specimen free span to the beam section height decreases, the shear stresses occurring in the beam section having parabolic tendons are lower than those of beams with straight tendons. This finding provides guidance to structural engineers in the preliminary design of structural systems.

Keywords: finite element; flexural capacity; post-tensioning; tendon layout

1 INTRODUCTION

As people began to live on earth, they were faced with the fact that they had to meet their basic needs such as eating, drinking, shelter, and protection. Human beings have built many structures such as shelters, warehouses, roads, water channels, bridges, and viaducts to meet these needs. While building these structures, they used natural building materials such as trees, stones, and soil, which they could easily find in their surroundings. Due to the inadequacies in the various strength and durability properties that these materials can provide, some restrictions (such as span, and height) have been made in the structures. With the development of technology, new materials have been constantly produced and existing materials have been improved to create stronger and more durable new building materials. Thanks to the physical and mechanical possibilities provided by developed materials (such as concrete, steel, and composite materials) and new construction techniques, building taller structures, bridges, and viaducts that cross wider spans has become possible.

One of the construction techniques used when it comes to the construction of large-span bridges and viaducts is pre-stressed reinforced concrete structural systems. Pre-stressing is the application of a force suitable for the desired purpose to the structural system before external loading. The origin of this construction technique dates back to ancient times. This technique has been used in many areas such as the manufacture of large wooden barrels that people use to store liquids and the construction of wooden wheels [1].

The spans that can be crossed with classical reinforced concrete beams are limited. As the span of the structural system increases, it is necessary to use reinforced concrete beams with larger cross-sections. Since concrete is a heavy building material, the growth of the sections causes the load, which we define as the useful load, to decrease. As a result, it is necessary to enlarge the cross-sections of the structural system in order to carry the payloads foreseen in the projects. As a result of the load affecting the structural systems and the resulting cycle of providing sufficient cross-section, we inevitably encounter heavy load-bearing systems. For this reason, the technique of carrying payloads with smaller cross-section beams has been the subject of constant research.

Pre-stressed reinforced concrete systems are divided into two parts: pre-tensioned systems and post-tensioned systems, according to the order of application of the tensioning process. In pre-tensioned systems, the tensioning of the tendons is done before the concrete is poured, and after the concrete reaches sufficient strength, the tendons are cut and the applied tension is transferred to the reinforced concrete structural system. Therefore, it is not possible to give a tendon form other than the straight tendon form in these systems. In post-tensioning systems, tendon sheaths are placed in the molds before the concrete is poured. After the concrete is poured, the steel tendons are passed through the sheaths, and the tensioning process is applied. For this reason, since the tensioning process is done later in post-tensioning systems, it is possible to give different tendon forms other than the straight tendon form (such as parabola, or triangle) [2-4].

After the pre-tensioning tendons are tightened and the load is transferred to the concrete, tension losses occur as the tendons loosen. Pre-stressing losses are evaluated in two parts: short-term and long-term losses. Short-term losses (anchor losses, elastic shortening, and friction losses) occur during load transfer to the tendons. Long-term losses occur from the rheological properties of concrete (creep and shrinkage). It is difficult to determine long-term losses and is only possible with long-term experimental studies [5].

By using pre-stressed structural systems, it is possible to cross large spans with reinforced concrete structural systems with smaller cross-sections. Observing and examining the long-term behaviour of structures is extremely important in terms of developing designs and reducing damages [6-10]. Since the cracks that form under service loads in these structural systems close after the load is removed, leakage and corrosion problems occur less than in normal reinforced concrete systems. This extends the service life of pre-stressed structural systems. Since pressure is applied to the sections with a tensioning system

during pre-tensioning, higher-strength concrete must be used compared to normal reinforced concrete systems.

Many numerical models have been presented to simulate the mechanical behavior of various structure members [11-17]. These numerical models mostly employ the finite difference method (FDM) or finite element method (FEM) for analysis [18-19]. In addition, the structural behavior of reinforced concrete structural elements such as beams and columns or the strengthening of damaged reinforced concrete members can be analyzed with FEM [20-24].

Within the scope of this study, first of all, six test specimens with a total dimension of 200 × 300 × 4400 mm were produced, two of which (NB/1-2) were made of normal reinforced concrete and the other four (POSTTENST/1-2, POSTTENP/1-2) were produced using the post-tensioning technique. In the (POSTTENST/1-2) specimens, the sheath through which the post-tensioning tendon will pass was placed straight, and in the (POSTTENP/1-2) specimens, the sheath was placed parabola, in line with the beam length section before the concrete was poured. The specimens were cured in the laboratory, covered and kept moist, for 28 days. After the specimens reached sufficient strength, the post-tensioning tendon was passed through the sheaths in straight form to the (POSTTENST/1-2) specimens, and the post-tensioning tendon was passed through the sheaths in parabola form to the (POSTTENP/1-2) specimens. Anchor elements were placed at the tendon ends of the post-tensioned specimens and post-tensioning force was applied with the hydraulic piston. A four-point bending test was performed on the specimens. During the experiment, the load applied to the specimens and the displacements in the middle of the beam were measured and recorded. Additionally, the specimens were observed and the cracks formed on the beam and the crack formation loads were written. After the experiments were completed, the data obtained were evaluated and the results were interpreted.

The study is important in that it highlights the superior aspects of bending and ductility capacities of structural systems strengthened with the post-tensioning technique compared to unstrengthened (normal) reinforced concrete structural systems. As a result of the experiments, it was determined that beams strengthened with straight and parabolic steel tendons could carry approximately 62% more load and behave approximately 65% more ductile than unstrengthened beams. The test specimen was modelled by the non-linear finite element method and compared with the experimental test results. The parametric analysis showed that the parabola tendon form is more effective in reducing the shear stresses occurring in the sections compared to the straight tendon form, as the ratio of the beam free span to the beam height (l/h) decreases. This situation is extremely important in terms of guiding engineers in the preliminary design of structural systems to be produced with the post-tensioning technique.

2 MATERIALS AND METHOD

2.1 Material Properties

In order to examine the effects of the geometric form of the post-tensioning tendon on the bending capacity, ductility capacity, and failure modes of the beam, six simply supported reinforced concrete beams were tested in the Structural and Earthquake Engineering Research Laboratory of Harran University Faculty of Engineering. The materials and their amounts used in the concrete mixture are shown in Tab. 1.

Table 1 Properties of concrete mixture

Cement / kN/m^3	Water / kN/m^3	Water/ Cement	Chemical Additive / kN/m^3	River sand / kN/m^3	Basalt / kN/m^3
4	1.64	0.41	0.08	4.25	15.1

In the production of all test specimens, Portland CEM I 52.5 N type cement, river sand, and basalt aggregate with the largest grain diameter of 16 mm were used according to TS EN 197-1 [25] standard. C55/67 concrete was used to produce the beams. The average cube (150 × 150 × 150 mm) compressive strength of the concrete used was determined to be 67 MPa in accordance with the TS EN 12390-3 [26] standard. The cross sections of all beams used in the experiments are 200 × 300 mm and their span is 4400 mm long.

Table 2 Properties of post-tensioning tendon

Diameter / mm	Cross sectional area / mm^2	Yield strength / MPa	Ultimate strength / MPa	Modulus of elasticity / MPa	Elongation at rupture / %
15.24	140	1676	1860	190000	3.5

Post-tensioning tendons are made of high-strength, low-relaxation multi-strand steel. The properties of the tendon are shown in Tab. 2. In the test specimen beams, in accordance with the TS 500 [27] standard, 12 mm diameter B420C ribbed rebar was placed as longitudinal reinforcement and 8 mm diameter shear reinforcement made of the same rebar was placed at a distance of 150 mm along the entire beam. The design parameters of the beams are summarized in Tab. 3.

Table 3 Design parameters of beams

Beams	Tendon diameter / mm	Tendon Layout	Rebar ratio / %	Stirrup	Post-tensioning force / kN
NB/1-2	-	-	0.94	Φ8/150	-
POSTTENST/1-2	1Φ15.24	Straight	0.94	Φ8/150	106
POSTTENP/1-2	1Φ15.24	Parabolic	0.94	Φ8/150	106

Within the scope of the research, post-tensioned reinforced concrete beams were produced in accordance with the TS 3233 [28] standard. The effect of the steel tendon forms placed on these beams to apply post-tensioning on the bending and ductility capacities of the beams was investigated. Straight and parabola tendon forms, which are most commonly used in practice, were compared with each other in terms of the bending and ductility capacity of the beams and the largest displacement amounts occurring in the middle of the beam. For this purpose, six beam specimens with dimensions of 200x300x4400 mm were produced in the study. Among these beam specimens, NB/1 and NB/2 were produced as normal reinforced concrete beams, and the other four beam

specimens were produced by stretching the tendons placed in the beam section with the post-tensioning method. The descriptions of the specimens in the photographs are written in Turkish (NK/1-2, ARDGD/1-2, and ARDGP/1-2). In the production technique of post-tensioned beams, after the reinforced concrete reinforcements are placed in the beam formwork, sheaths are placed in the position where the post-tensioning tendons will be passed. After the concrete pouring was completed and sufficient strength was reached, the post-tensioning tendons were passed through the sheaths, and the production process was completed by applying tension to the tendons. Among these beam specimens, in the research, POSTTENST/1 and POSTTENST/2 beams were created with straight tendon form, and POSTTENP/1 and POSTTENP/2 beams shown in Fig. 1 were created with parabola tendon form.

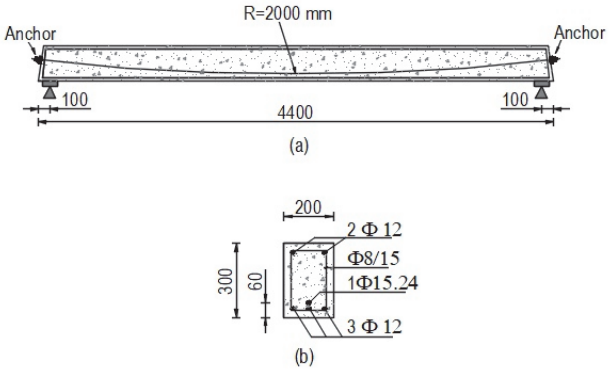

Figure 1 (a) Beam longitudinal section, (b) beam cross-section and reinforcement details (dimensions are given in mm)

2.2 Experimental Program and Testing Stages

A four-point bending test was performed on all test specimens. In this experimental setup, the specimen is contacted from four points as shown in Fig. 2. Two of these points are located in the support area, while the other two are in the area where the load is applied. In experiments carried out in this way, only a constant bending moment occurs in the region between the loads applied to the specimens, and no shear force occurs. In this way, it is possible to clearly examine the cracks where a constant bending moment occurs in a wide area where loads are applied [29].

The load applied to the simply supported beam and 1400 mm long rigid steel beam placed on the test specimen was distributed equally on the specimen as two single loads. The experiments were carried out with displacement control by loading the specimens with a loading speed of 1.2 mm/min through a hydraulic actuator until all the specimens collapsed. Linear Voltage Differential Transformers (LVDT) were placed under the beams in the middle of the span in order to measure the amount of displacement occurring there. The experimental setup is shown in Fig. 3. The displacement in the middle of the span and the applied load during the test were automatically recorded in the computer system through the data acquisition unit. Tests of normal beam the (NB) and post-tensioned (POSTENST, POSTENP) beams were continued until the displacement in the middle of the span exceeded 40 mm and the experiments lasted approximately 35 minutes. The crack directions formed during the test were marked on the beam and the load values were written gradually. Marking operations were completed before the load applied to the beam was removed.

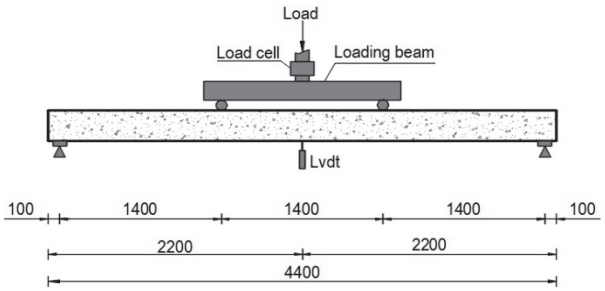

Figure 2 Schematic view of four-point bending test setup (dimensions are in mm)

Figure 3 Test specimen and four-point bending test setup

3 ANALYSIS AND RESULTS

3.1 Failure Mechanism

During the loading process, the occurrence and development of cracks were monitored in all test specimens. As stated above the paths of the cracks were marked on the beam surfaces and the occurred loads were written. Schematic drawings of the typical cracking patterns of control (NB) and post-tensioned beam specimens (POSTTENST-POSTTENP) having geometrically different tendons are shown in Fig. 4, Fig. 5, and Fig. 6.

In all beams, the first flexural cracks were observed at the midspan of specimens on the tension side of the constant moment region. When the load increased the cracks developed along the constant moment region. The shear cracks formed in the shear span for post-tensioned beam specimens having straight tendons while this type of cracks did not occur in the post-tensioned beams with the parabolic tendon (POSTTENP/1, POSTTENP/2) due to its geometrical shape. Because the parabolic tendon was detailed as diagonal in the shear span. In all beam specimens, failure occurred at the maximum load. After failure, the beams carried practically no load. Cracks consisted of vertical flexural cracks in the pure bending region regardless of tendon shape as well as NB specimens. Furthermore, cracks outside the constant moment region progressed as flexural cracks at the lower load grade compared to the cracks that occurred at pure bending region but converted into inclined shear cracks at higher load levels in all beams except for (POSTTENP/1, POSTTENP/2) specimens having parabolic tendon.

Figure 4 Shear and bending cracks (a) NB/1, (b) NB/2

Figure 5 Flexural and shear cracks of straight post-tensioned beam (a) POSTETNST/1, (b) POSTENST/2

In addition to all these, many cracks with smaller widths were observed on the post-tensioned beam specimens having straight/parabolic tendons compared to normal beam specimens. Also, the post-tensioned reinforced concrete beams having parabolic tendons had more cracks than those having straight tendons (Fig. 5a, Fig. 5b and Fig. 6a, Fig. 6b). On the other hand, the failure of the post-tensioned specimens having straight/parabolic tendons was gradual and in a ductile manner, especially for the parabolic tendon reinforced concrete beam specimens. This condition may be attributed to a great number of cracks on the tension side of these specimens under flexural loading.

Figure 6 Flexural and shear cracks of parabolic post-tensioned beam (a) POSTTENP/1, (b) POSTTENP/2

3.2 Load Displacement Behaviour of Beam Specimen

The load-displacement graphs of reinforced concrete NBs and POSTTEN beams were compared with each other, and the load-displacement curves are shown in Fig. 7. For NB specimens, it was observed that the first crack started to form around 13 kN. In POSTTENST-POSTTENP specimens, the first crack formation occurred around a load of 36 kN. It was observed that the initial crack load in post-tensioned specimens was greater than that of NBs (approximately 2.7 times). The fact that the initial stiffness of POSTTEN specimens is higher than that of NB specimens in the behaviour until the formation of the first crack shows that the beams will deflect less and fatigue is less under the effect of service loads. This also means that the useful life of POSTTEN specimens will be longer.

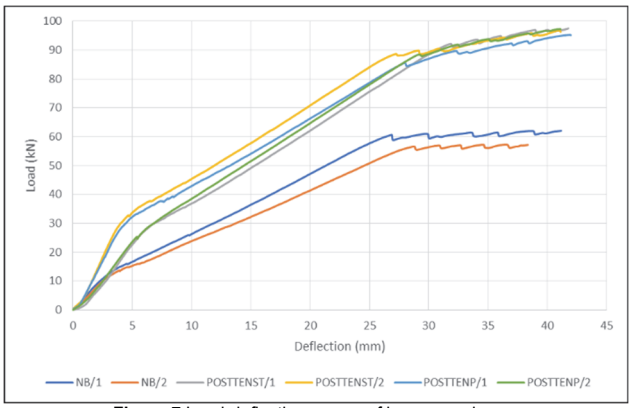

Figure 7 Load-deflection curves of beam specimens

It is clearly seen from examining Fig. 7 that the collapse loads corresponding to the mid-span deflections

of the non-post-tensioned NB specimens are smaller than the collapse loads of all the post-tensioned specimens. This is an expected and normal result. While the collapse loads of all POSTTENST and POSTTENP specimens were between 95 kN and 98 kN, as shown in Fig. 8, the collapse loads of NBs were between 55 kN and 65 kN. It was determined that post-tensioned (POSTTENST-POSTTENP) specimens carried approximately 62% more load than normal beam (NB) specimens.

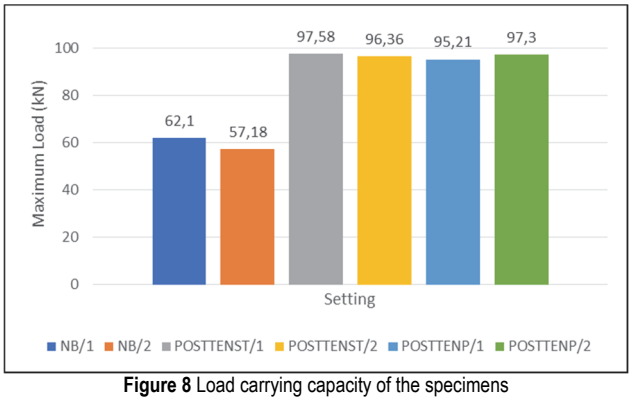

Figure 8 Load carrying capacity of the specimens

Table 4 Bending test results of the specimens

Specimen Group	Specimen Name	Ultimate Load / kN	Energy dissipation capacity / kNmm	Increasing rate of energy dissipation capacity / %
NB	NB/1	62.1	1760	-
	NB/2	57.2	1440	
POSTTENST	POSTTENST /1	97.6	2560	65
	POSTTENST /2	96.4	2730	
POSTTENP	POSTTENP/1	95.2	2690	64
	POSTTENP/2	97.3	2545	

The energy dissipation ability of building elements under applied loads is described as ductility. The ductility of a structure is directly related to the ductility of its constituent structural members. Therefore, obtaining ductile structures, which are extremely important in terms of earthquake behaviour, is only possible by creating ductile structural members. Since ductile structures have the ability to make large displacements before collapsing, they inform us before the structure collapses. This situation is extremely important in reducing the loss of life.

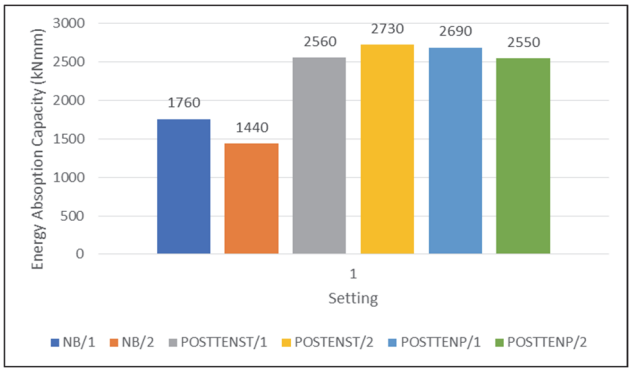

Figure 9 Energy dissipation capacities of the specimens

The energy dissipation capacities of the specimens were determined by calculating the total areas under the load-deflection curves. After calculating the areas between two consecutive deflection points, they were added together to determine the total area between the load-deflection curves. The energy capacities of the specimens and their comparison with each other based on NB specimens are shown in Tab. 4 and Fig. 9. It has been determined that post-tensioned POSTTENST-POSTTENP specimens absorb approximately 65% more energy than NB specimens.

3.3 Finite Element Models and Comparing with the Experimental Result

In this section, the load-deflection curves obtained from the test specimens are compared with the analysis results obtained from the finite element models of the specimens. The analysis of the test specimens was modelled with the nonlinear finite element method using the Abaqus/CAE program [30]. Modelling C3D8R (8-node linear single element) finite element was chosen because it is a suitable element type for the examination and evaluation of cracks [31-32]. The mesh element size that would provide sufficient accuracy in the analysis was determined as 50 mm, considering the computer capacity. In modelling, the "concrete damage plasticity model" was adopted for concrete, and the two-dimensional "Truss" element model was adopted for reinforcement and tendon. The CDP model is frequently used in nonlinear material definition research [33-34]. A finite element interaction was created by creating contact connection elements between concrete and reinforcement. Tension losses in the post-tensioning tendon were neglected in the analysis.

The modelling was based on the four-point bending test, as shown in Fig. 10, as in the experimental setup. Boundary conditions and locations of loading points were chosen to be the same as in the experimental study. The analyses were carried out in a displacement-controlled manner, by applying the load to the specimens as two singular forces at 1/3 of the free span of the beam. The stress distribution of the NB/1 specimen is shown in Fig. 11 as an example. It is noteworthy that shear stresses are concentrated in the region close to the support area.

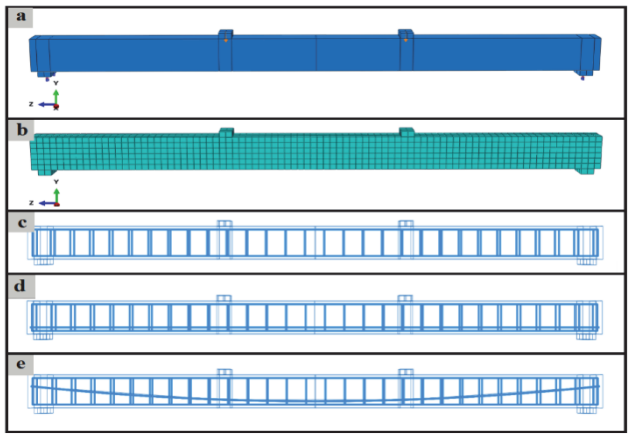

Figure 10 Finite element models: a) Details of the test specimen, b) finite element mesh, c) normal beam specimen, d) straight tendon post-tensioning specimen, e) parabola tendon post-tensioning specimen

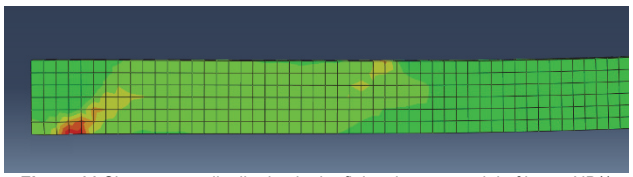

Figure 11 Shear stress distribution in the finite element model of beam NB/1

The experimental results obtained from the specimens and the finite element method results were compared with each other. Load-deflection graphs of the results of the experiments and analytical investigation are shown in Fig. 12.

The average results of the experimental test specimens and the energy dissipation capacities and ultimate load obtained from the finite element analysis results are given in Tab. 5.

Table 5 Experimental test and finite element analysis results for specimens

		NB	POSTTENST	POSTTENP
Ultimate load / kN	Experimental	59.64	96.97	96.21
	Finite element	58.12	94.64	97.11
Energy dissipation capacity / kNmm	Experimental	1603	2644	2618
	Finite element	1734	2342	2303

It was observed that there was a difference of approximately 2% between the test results and the finite element analysis results in the load-carrying capacities and approximately 8% in the energy dissipation capacities. It is understood that these values are in good agreement with the experimental results and the finite element analysis results. When the results obtained are evaluated, they show the meticulousness shown in the design of the experimental setup, the measurements made, and the preparation of the specimens.

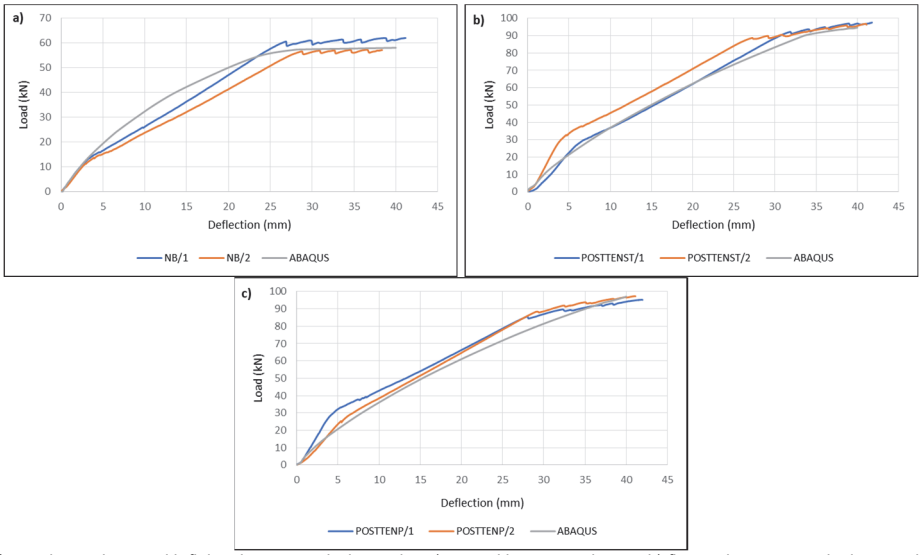

Figure 12 Comparison of experimental tests with finite element analysis results: a) normal beam specimens, b) flat tendon post-tensioning specimens, c) parabola tendon post-tensioning specimens

3.4 Parametric Analysis

The shear strength of pre-stressed reinforced concrete sections is much higher than normal reinforced concrete sections. The main reasons for this can be stated as the high quality of the concrete, the increase in friction due to the pre-stressing force, and the reduction of shear forces caused by vertical loads by the forces in the opposite direction. The decrease in shear forces in the load-bearing system shows its effect in the form of a decrease in the shear stresses occurring in the sections. In this section, it is investigated how this effect is affected by the change in the ratio of the beam free span (l) to the beam cross-section height (h). It has been investigated at which values of the l/h ratio the parabolic tendon geometric form can provide a significant advantage compared to the straight tendon form in terms of reducing the maximum shear stress. For this purpose, three different rectangular cross-section beams with l/h ratios of 12.66, 14, and 16 were modelled using the Abaqus/CAE program, keeping the same material properties used in the experimental part.

Table 6 Maximum shear stresses of the models

Model name	Clear span (l) / m	Width (b_w) / mm	Height (h) / mm	l/h	Post-tensioning force / kN	Max. shear stress ($\tau_{max.}$) / MPa		Variation between tendon layout / %
Tendon form	-	-	-	-	-	Parabolic	Straight	
Model 1	9.5	500	750	12.66	980	6.04	12.86	53
Model 2	4.2	200	300	14	106	14.92	16.56	10
Model 3	24	800	1500	16	3700	12.71	13.96	9

In creating and analysing the models, attention was paid to the issues explained in Chapter 3.3. In all parabola and straight tendon form beams, the dead load (g) was taken as 32 kN/m, and the live load (q) was taken as 23.5 kN/m. The largest shear stresses occurring in the beams under the influence of these loads and the change

values in these stresses are compared in Tab. 6.It is understood that as the ratio of the beam free span to the beam height (l/h) decreases, the maximum shear stresses occurring in the sections of the parabolic tendon form decrease compared to the straight tendon form. This will be useful to structural engineers in the preliminary design of structural systems in the form of parabola tendons to be produced with the post-tensioning technique.

4 CONCLUSIONS

To examine the effect of tendon geometry on the bending capacity of beams in carrier systems produced with the post-tensioning technique, six reinforced concrete beams with cross-sectional dimensions of 200 × 300 mm and a length of 4400 mm were produced. Displacement-controlled loading was performed on the beams with a four-point loading test and the displacement in the middle of the span was measured. The cracks that occurred on the specimen during the experiment were drawn and the load values at the time the crack occurred were written on the specimens. The results obtained from the evaluation of the test results are summarized below.

Considering the displacements in the middle of the beam, the unstrengthened normal beams (NB/1 and NB/2), beams with straight tendons (POSTTENST/1 and POSTTENST/2), and beams with parabolic tendons (POSTTENP/1 and POSTTENP/2) of the twin beam specimens cast in short time intervals, each pair collapsed at a force level close to each other. This is largely the result of the small beam heights and is also an indication of the care and meticulousness shown in the production of the specimens.

The specimens to which the post-tensioning technique was applied (POSTTENST/1, POSTTENST/2 and POSTTENP/1, POSTTENP/2) exhibited very similar behaviour to each other. Shear cracks occurred less in beam specimens produced with parabolic tendon form (POSTTENP/1and POSTTENP/2) than in beam specimens produced with straight tendon form (POSTTENST/1 and POSTTENST/2). This situation shows the contribution of the parabola tendon form in reducing the shear stresses in the beam.

Post-tensioned specimens carried approximately 62% more load and absorbed 65% more energy than normal reinforced concrete specimens. This situation has once again shown that it is possible to cross larger spans with smaller reinforced concrete sections using the post-tensioning technique. In addition, in countries at risk of earthquakes, this ratio is extremely important in reducing structural damage and loss of life caused by earthquakes.

At the end of the experimental test, it was determined that after the load on the specimens was removed, the rate of closure of cracks in the post-tensioned specimens was higher and faster than in normal reinforced concrete specimens. This will reduce the contact of the structural system with the external environment more quickly and will result in less corrosion in the reinforcement. Thus, the service life of the structural systems will be increased.

In the study, the specimens were also modelled and analyzed by the ABAQUS finite element method. The study is limited to three finite element models with different dimensions. It has been observed that the results obtained are in great consistency with the experimental results.

The parabola-shaped tendon form used in post-tensioned beams reduces the shear forces in the system thanks to the counter-load effect created in the opposite direction to the external loads. Reducing the shear forces in the beam will ensure that the shear stresses in the sections remain at lower levels. In the parametric analysis, it was seen that this effect increased as the l/h ratio decreased. These results guide structural engineers in the preliminary design of post-tensioned beams. The fact that the parabolic tendon form reduces shear stresses will allow sections to be created using less shear reinforcement. This will create an advantage in terms of labour and economic production. It is thought that the results obtained in this research study will be useful in determining the specimen sizes in future post-tensioned beam test studies.

Acknowledgments

This research was supported by the Harran University Scientific Research Projects Coordination Unit of Turkey (HUBAP project numbers: 18141)

5 REFERENCES

[1] Keyder, E. (2013). Öngerilmeli Beton, Seçkin Yayıncılık ve Dağıtım.
[2] Şener, S. (2006). Öngerilmeli Beton, Alp Yayınevi.
[3] Tan, K. H. (2014). Beam strengthening by external post-tensioning: Design recommendations. *The IES Journal Part A: Civil & Structural Engineering, 7*(4), 219-228.
[4] Naser, A. F. (2018). Optimum design of vertical steel tendons profile layout of post-tensioning concrete bridges: fem static analysis. *ARPN Journal of Engineering and Applied Sciences, 13*(23), 9244-9256.
[5] Rodrigues, C., Felix, C., Lage, A., & Figueiras, J. (2010). Development of a long-term monitoring system based on FBG sensors applied to concrete bridges. *Engineering Structures, 32*(8), 1993-2002. https://doi.org/10.1016/j.engstruct.2010.02.033
[6] Robertson, I. N. (2005). Prediction of vertical deflections for a long-span prestressed concrete bridge structure. *Engineering Structures*, *27*(12), 1820-1827. https://doi.org/10.1016/j.engstruct.2005.05.013
[7] Tong, G., Zheheng, C., Shuo, L., & Ruigen, Y. (2018). Monitoring and analysis of long-term prestress losses in post-tensioned concrete beams. *Measurement, 122*, 573-581. https://doi.org/10.1016/j.measurement.2017.07.057
[8] Y., T-H., L., H-N., & G., M. (2013). Experimental assessment of high-rate GPS receivers for deformation monitoring of bridge. *Measurement, 46*(1), 420-432. https://doi.org/10.1016/j.measurement.2012.07.018
[9] Y., T-H., L., H-N., & G., M. (2013). Wavelet-based multi-step filtering method for bridge health monitoring using GPS and accelerometer, *Smart Structures and Systems, 11*(4), 331-348. https://doi.org/10.12989/sss.2013.11.4.331
[10] Y., T-H., L., H-N., & G., M. (2013). Recent research and applications of GPS-based monitoring technology for high-rise structures. *Structural control and health monitoring, 20*(5), 649-670. https://doi.org/10.1002/stc.1501
[11] Sezen, H., Acar, R., Dogangun, A., & Livaoglu, R. (2008). Dynamic analysis and seismic performance of reinforced concrete minarets. *Engineering Structures, 30*(8), 2253-2264. https://doi.org/10.1016/j.engstruct.2007.11.005

[12] Muvafik, M. (2014). Field investigation and seismic analysis of a historical brick masonry minaret damaged during the Van Earthquakes in 2011. *Earthquakes and Structures, 6*(5), 457-472. https://doi.org/10.12989/eas.2014.6.5.457
[13] Koseoglu, G. C. & Canbay, E. (2015). Assessment and rehabilitation of the damaged historic Cenabı Ahmet Pasha Mosque. *Engineering Failure Analysis, 57*, 389-398. https://doi.org/10.1016/j.engfailanal.2015.08.015
[14] Bilgin, H., Shkodrani, N., Hysenlliu, M., Ozmen, H. B., Isik, E., & Harirchian, E. (2022). Damage and performance evaluation of masonry buildings constructed in 1970s during the 2019 Albania earthquakes. *Engineering Failure Analysis, 131*, 105824. https://doi.org/10.1016/j.engfailanal.2021.105824
[15] Işık, E., Antep, B., Büyüksaraç, A., & Işık, M. F. (2019). Observation of behavior of the Ahlat Gravestones (TURKEY) at seismic risk and their recognition by QR code. *Structural Engineering and Mechanics, an Int'l Journal, 72*(5), 643-652.
[16] Bilgin, H. (2024). Effects of near-fault and far-fault ground motions on nonlinear dynamic response and seismic damage of masonry structures. *Engineering Structures, 300*, 117200. https://doi.org/10.1016/j.engstruct.2023.117200
[17] Demir, A. & Altıok, T. Y. (2021). Numerical assessment of a slender structure damaged during October 30, 2020, İzmir earthquake in Turkey. *Bulletin of Earthquake Engineering, 19*(14), 5871-5896. https://doi.org/10.1007/s10518-021-01197-8
[18] Işık, E., Avcil, F., Harirchian, E., Arkan, E., Bilgin, H., & Özmen, H. B. (2022). Architectural characteristics and seismic vulnerability assessment of a historical masonry minaret under different seismic risks and probabilities of exceedance. *Buildings, 12*(8), 1200. https://doi.org/10.3390/buildings12081200
[19] Avcil, F., Işık, E., Bilgin, H., & Özmen, H. B. (2022). TBDY-2018'de Verilen Tasarım Spektrumlarının Anıtsal Yığma Yapı Sismik Davranışına Etkisi. *Adıyaman Üniversitesi Mühendislik Bilimleri Dergisi, 9*(16), 165-177. https://doi.org/10.54365/adyumbd.1051120
[20] Fenerci, A., Binici, B., Ezzatfar, P., Canbay, E., & Ozcebe, G. (2016). The effect of infill walls on the seismic behavior of boundary columns in RC frames. *Earthquakes and structures, 10*(3), 539-562. https://doi.org/10.12989/eas.2016.10.3.539
[21] Shendkar, M. R., Kontoni, D. P. N., Mandal, S., Maiti, P. R., & Gautam, D. (2021). Effect of lintel beam on seismic response of reinforced concrete buildings with semi-interlocked and unreinforced brick masonry infills. *Infrastructures, 6*(1), 1-18. https://doi.org/10.3390/infrastructures6010006
[22] Ebadi-Jamkhaneh, M., Homaioon-Ebrahimi, A., & Kontoni, D. P. N. (2021). Numerical finite element study of strengthening of damaged reinforced concrete members with carbon and glass FRP wraps. *Computers and Concrete, 28*(2), 137-147.
[23] Zhulegu, E. & Bilgin, H. (2012). Seismic performance assessment of a reinforced concrete building designed using the albanian seismic code. *Proceedings of the Eleventh International Conference on Computational Structure*.
[24] Ebadi-Jamkhaneh, M., Kontoni, D. P. N., & Homaioon Ebrahimi, A. (2024). Assessment of Different Methods for Enhancing Progressive Collapse Resistance of Irregular Reinforced Concrete Buildings Using Pushdown Analysis. *Arabian Journal for Science and Engineering,* 1-23. https://doi.org/10.1007/s13369-024-08847-4
[25] Turkish Standard Institute. (2012). TS EN 197-1. Cement-part 1: Composition, specification and conformity criteria for common cements, Ankara: TSI.
[26] Turkish Standard Institute. (2019).TS EN 12390-3.Testing hardened concrete - Part 3: Compressive strength of test specimens, Ankara: TSI.
[27] Turkish Standard Institute. (2000).TS 500.Requirements for design and construction of reinforced concrete structures, Ankara: TSI.
[28] Turkish Standard Institute. (1979). TS 3233 Building Code Requirements for Prestressed Concrete. Ankara: TSI.
[29] Abdulkadir, G. (2020). *Investigation Of The Usability Of Rectangular And T-Section Prefabricated Cage Reinforced Beams Under Flexural Loads*. Ph.D. Thesis, Kahramanmaras Sutcu Imam University, Kahramanmaras, Turkey.
[30] Abaqus. (2014). ABAQUS user's manual version 6.14-1, Hibbitt, Karlsson & Sorensen, Inc., Providence, RI, USA.
[31] Fanning, P. (2001).Nonlinear models of reinforced and post-tensioned concrete beams. *Electronic Journal of Structural Engineering, 1*(2), 111-119. https://doi.org/10.56748/ejse.1182
[32] Mali, P. R. & Datta, D. (2020). Experimental evaluation of bamboo reinforced concrete beams. *Journal of Building Engineering, 28*, 101071. https://doi.org/10.1016/j.jobe.2019.101071
[33] Pekgökgöz, R. K. & Avcil, F. (2021). Effect of steel fibres on reinforced concrete beam-column joints under reversed cyclic loading. *Građevinar, 73*(12), 1185-1194. https://doi.org/10.14256/JCE.3092.2020
[34] Avcil, F., Izol, R., Gürel, M. A., Arkan, E., & Mollamahmutoğlu, Ç. (2023). Efficiency of Buttress Form on the Out-of-plane Resistance of Masonry Walls Subjected to Vault Thrust. *Tehnički vjesnik, 30*(4), 1039-1046. https://doi.org/10.17559/TV-20220918185452

Contact information:

Recep Kadir PEKGÖKGÖZ, Associate Professor, PhD
(Corresponding author)
Harran University, Department of Civil Engineering,
Şanlıurfa, Turkey
E-mail: recepkadir@harran.edu.tr

Gamze İZOL, Graduate Student, MSc
Harran University, Department of Civil Engineering,
Şanlıurfa, Turkey
E-mail: izolgamze@gmail.com

Fatih AVCİL, Assistant Professor, PhD
Bitlis Eren University, Department of Civil Engineering,
13000 Bitlis/Turkey
E-mail: favcil@beu.edu.tr

M. Arif GÜREL, Professor, PhD
Harran University, Department of Civil Engineering,
Şanlıurfa, Turkey
E-mail: agurel@harran.edu.tr